

A method for extreme data reduction of Acoustic Emission (AE) data with application in machine failure diagnosis

Cristián Molina Vicuña¹ and Christoph Höweler²

¹Laboratorio de Vibraciones Mecánicas, Universidad de Concepción
Edmundo Larenas 270 int., Concepción, Chile

²VIAMIS - Industrial Services & Research; Condition Based Maintenance
Gasborn 33, 52062 Aachen, Germany
{crimolin@udec.cl, christoph.hoeweler@viamis.de}

Abstract

The use of AE in machine failure diagnosis has increased over the last years. Most AE-based failure diagnosis strategies use digital signal processing and thus require the sampling of AE signals. High sampling rates are required for this purpose (e.g. 2 MHz), which leads to streams of large amounts of data. This situation is aggravated if fine resolution and/or multiple sensors are required. These facts combine to produce bulky amounts of data –typically in the range of GBytes,– for which sufficient storage space and efficient signal processing algorithms are required. This situation probably explains why, in practice, AE-based methods consist mostly in the calculation of scalar quantities such as RMS, Kurtosis, etc., and the analysis of their evolution in time. While the scalar-based approach offers the advantage of maximum data reduction; it has the disadvantage that most part of the information contained in the raw AE signal is lost unrecoverably. This work presents a method offering extreme data reduction, while keeping the most important information conveyed by the raw AE signal, which is useful for failure diagnosis purposes. The proposed method is very simple: it consist on the construction of a synthetic, unevenly sampled signal which envelopes the AE bursts present on the raw AE signal in a triangular shape. The constructed signal –which we call *TriSignal*– also permits the estimation of most scalar quantities typically used. But more importantly, it contains the information of the time of occurrence of the bursts, which is key for failure diagnosis. Furthermore, we show how the *TriSignal* can be used to compute the *TriSpectrum*, an estimator of the frequency content of the AE envelope.

1 Introduction

During the last decades we have experienced an increase in the use of AE for condition monitoring of machines [1]. The most important advances have been made in the problem of bearing failure detection. In this case, the detection is based on the major differences between the AE generated by healthy and faulty bearings. In the first case, the AE signal has a noise-like shape; whereas when a fault develops, the resulting AE contains a number of bursts. Although this is the particular case for bearings, there are other elements in which a failure does also result in AE bursts; these include gears [2][3][4][5] and cracks [6]. This situation justifies why the interest has been focused on the detection of the presence of the bursts in the AE signal.

In cases where the fault is the only source of burst-type AE, the calculation and trending of scalar values (e.g. Kurtosis, RMS) is commonly sufficient for this task. This is the case of bearings, and probably explains why the majority of research in this subject has relied on this scalar-based approach [7][8][9][10]. Some investigators have reported interesting advances including the correlation of the scalar quantities with the failure size [11][12]. Most of these researches use test benches comprising only bearings (one of them being the test object). Thus, the only source of burst-type AE is indeed the bearing fault. This is illustrated in Fig.1, where the AE measured on the bearing case of a bearing test bench such as the described are presented for the non-faulty and faulty case. The AE resulting from the bearing in good condition is a random signal presenting no recognizable bursts. Differently, a succession of bursts are evidenced when the faulty bearing (in this case outer race defect) is installed. The bursts are generated by the interaction of the rotating elements with the faulty

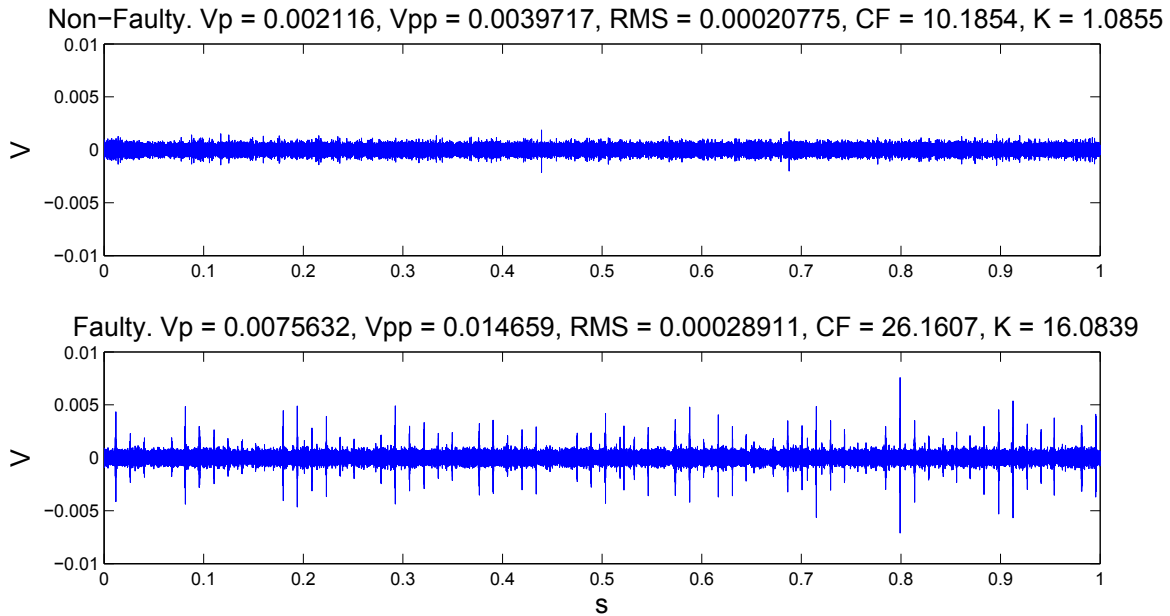


Figure 1: AE measured on the bearing case of a bearing test bench. (a) Non-faulty bearing. (b) Faulty bearing (outer race fault). Nomenclature of scalar values: V_p : peak; V_{pp} : peak-to-peak; RMS : Root Mean Square; CF : crest factor; K : Kurtosis.

zone. The plots in Fig.1 also include the magnitude of scalar values typically used. Note how all these values increase, thus evidencing the presence of the fault. As expected in a case like this, the Kurtosis is the most sensitive parameter. The advantage of the scalar based approach is that the scalar quantities can be calculated by hardware and, thus, can be recorded using low-cost data acquisition systems.

Based on the previous example one would not need a different method, since the scalar-based approach is sufficient for the detection of the fault. However, real machines do also include other mechanical components, being gear transmissions probably the most often found. Even though several questions regarding the behaviour of AE in gears still are subject of research, there is enough evidence of the burst-type AE generated as the (non-faulty) gear teeth mesh [5]. In a situation like this, the scalar quantities calculated from the AE measured on, for example, a gear transmission, would be largely influenced by the bursts coming from the gear tooth interactions. Hence, under the presence of a bearing fault, the scalar-based approach would only be successful if the bursts originated by the fault are large enough to produce recognizable changes in the scalar values. From our experience, this is rarely the case.

Consider the AE signal shown in Fig.2a, which was measured on the case of a planetary gearbox without failures. The figure also presents the values of the scalar quantities typically used. Figure 2b shows the situation for the AE measured on the same gearbox, but with a faulty planet gear (localized seeded defect). The only scalar quantities incrementing their values with respect to the non-faulty situation were the RMS (13.7%) and the Kurtosis (1.6%), but is arguable if this increase is sufficient to be indicative of the presence of the fault, since AE from gears are also sensitive to changes in load and speed [5]. Keep in mind, however, that the information related to the failure *is* present in the raw AE; it is only that the scalar values are not much sensitive to it. The problem is that this information can not be recovered from the scalar quantities; that is, the evidence of the presence of the failure is lost unrecoverably.

The previous examples illustrate the need for a different approach, capable of overcoming this situation. Recognizing that the succession of bursts present on the AE signal make it essentially a cyclostationary signal, a straightforward solution would be to scrutinize the frequency structure of the cyclic amplitude changes. Probably the best alternative to do this is by using the Spectral Correlation Density (SCD) or the Spectral Coherence (SCoh) [13], since both present the content of the amplitude changes in the frequency and cyclic frequency domain simultaneously. However, the computing costs of doing this (in terms of time consumption and processing requirements) might be too high for some applications.

The envelope spectrum is another cyclostationary tool which demands less computing costs, but is not as powerful as the SCD and SCoh [14]. In most cases, the envelope spectrum would probably be the best solution. However, the envelope spectrum it is still a vector containing a number of elements that can be large depending

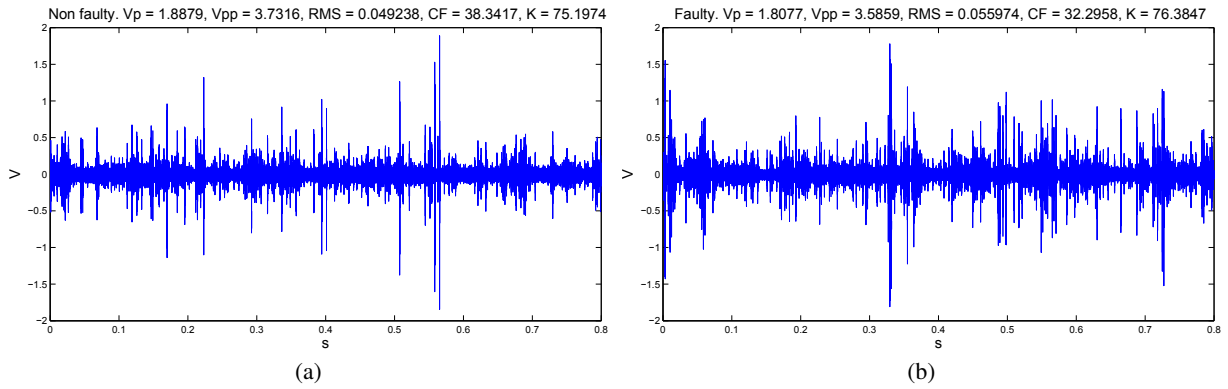


Figure 2: Acoustic emissions measured on a planetary gearbox (a) non-faulty. (b) Localized planet defect. Nomenclature of scalar values: V_p : peak; V_{pp} : peak-to-peak; RMS : Root Mean Square; CF : crest factor; K : Kurtosis.

on the resolution and maximum frequency. In some applications, the envelope might still be *expensive* in terms of storage requirements.

This work presents an alternative method offering extreme data-reduction possibilities, while keeping the most important information conveyed by the raw AE-signal, which is useful for machine failure diagnosis. Another advantage of the method is its simplicity. We present the method in the following sections.

2 The *TriSignal* method

One of the most important applications of AE in condition monitoring is in low-speed machinery. This is because at low speeds, the energy released due to the interaction of the elements under the presence of a fault is sometimes not sufficient to produce actual movements, but sufficient to produce acoustic waves. Thus, measurements from vibration sensors usually do not contain information related with the failure; whereas data from AE sensors have more chances of carrying this valuable information.

When dealing with low-speed machines, signals containing several shaft revolutions are normally needed to obtain the desired frequency resolution. For example, a resolution of 0.1 Order would be a typical choice for the analysis. If the shaft rotates at 1 Hz, then a 10 s long signal is must be recorded. If the sampling rate is 2 MHz and the double-precision format is used, then 160 MBytes of data are generated. The data amount grows when multiple channels and repetitive measurements are needed, as would be the case for typical continuous monitoring systems. Large storage capabilities would then be required to store the measurements. Moreover, the processing of such amount of data demands high computing requirements and efficient signal processing algorithms. In practice, all this results in expensive systems and is probably the reason why the scalar-based approach has prevailed, at the expenses of great information loss.

The proposed method was developed with the objective of keeping the most possible information relevant for failure diagnosis, which is contained in the raw AE signal, while offering large data reduction, thus providing a solution to the afore mentioned situation. The method consist in the construction of a synthetic, unevenly sampled signal, which envelopes the AE bursts present in the raw AE signal in a triangular shape, so that each burst in the signal is enveloped by a triangle, as shown in Fig.3a. Note from this figure that three coordinate pairs are needed for this purpose; however it is only required to obtain four scalar values from the AE signal. Three scalar values contain the time information descriptive of the burst: t_s^i is the start time of the burst; t_m^i is the time of maximum amplitude; and t_e^i is the time of burst end. The fourth scalar value (y_n^i) contains the maximum amplitude of the burst ($i = 1, 2, \dots$ is the burst index). The amplitude of the first and third coordinate pair are only required to close the triangle, hence they arbitrarily take the value of zero (i.e. $y_s^i = y_e^i = 0$). The *TriSignal* is then formed by the succession of all triangles enveloping the bursts in the AE signal, as presented in Fig.3b. From this definition, the *TriSignal* can be interpreted as an unevenly, undersampled envelope of the raw AE signal. Although the idea of the *TriSignal* might appear simplistic, we show in the next sections that it can be used to construct powerful tools for failure diagnostics.

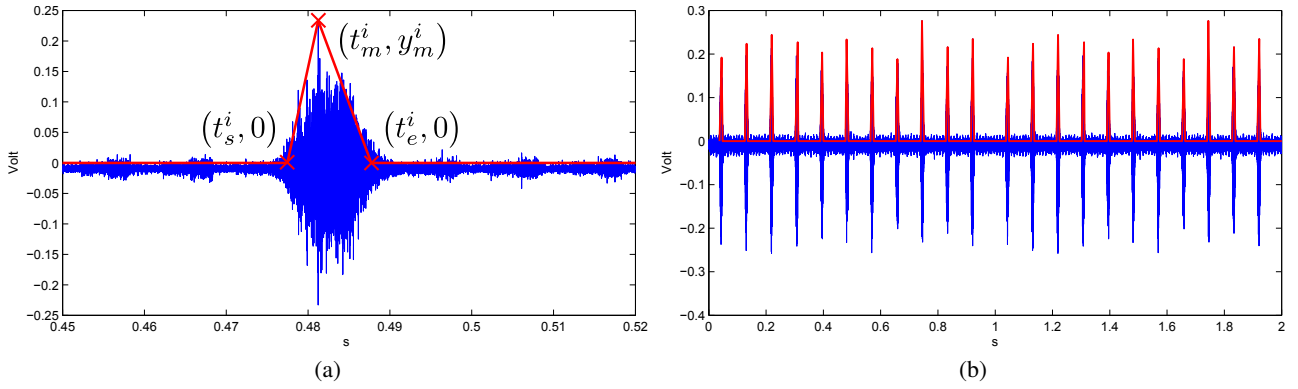


Figure 3: Construction of the *TriSignal*. (a) Enveloping a single burst in triangular shape. (b) The *TriSignal* (red) is formed by the succession of triangles enveloping the bursts in the raw AE signal.

2.1 Data reduction features

Let us consider we would like to determine the condition of a bearing rotating at 1 Hz. In order to do this a frequency resolution of 0.1 Hz has been chosen, for which an AE signal of length 10 s has been measured. The sampling rate is 1 MHz and the data is stored in double-precision format. Let us also suppose the bearing has an outer race defect and the BPFO is approximately 7 Hz. Table 1 resumes the storage requirements of the raw AE and the results of different processing techniques. In the case of the envelope, a downsampling factor of 200 has been considered.

| Item | Data amount | Data reduction |
|--------------------------|-------------|--|
| Raw AE (10 s) | 80 MByte | – |
| AE-Envelope (10 s) | 0.4 MByte | 99.500% w.r.t. raw AE |
| <i>TriSignal</i> (10 s) | 2.24 kByte | 99.440% w.r.t. AE-Envelope 99.997% w.r.t. raw AE |
| Scalar values (5 values) | 40 Byte | 98.214% w.r.t. <i>TriSignal</i> 99.990% w.r.t. AE-Envelope 99.999% w.r.t. raw AE |

Table 1: Storage requirements and data reduction.

Note in this case the AE-envelope performs greatly in terms of data reduction with respect to the raw AE (reduction of 99.500%). The *TriSignal* performs even better giving a further reduction of 99.440% (with respect to the AE-Envelope). As expected, the maximum reduction is obtained with the scalar-based approach. Table 2 shows the amount of data generated over a period of 1 month and 1 year, considering the case in which an AE-based continuous monitoring system is used. The system performs 2 measurements each day, each of 10 s, and has 4 channels. The large amounts of accumulated data could also add difficulties in the data handling and backup.

| Item | After 1 month | After 1 year |
|--------------------------|---------------|--------------|
| Raw AE (10 s) | 9.6 GByte | 116.8 GByte |
| AE-Envelope (10 s) | 48 MByte | 584 MByte |
| <i>TriSignal</i> (10 s) | 268.8 kByte | 3.3 MByte |
| Scalar values (5 values) | 4.8 kByte | 58.4 kByte |

Table 2: Accumulated data after a period of time.

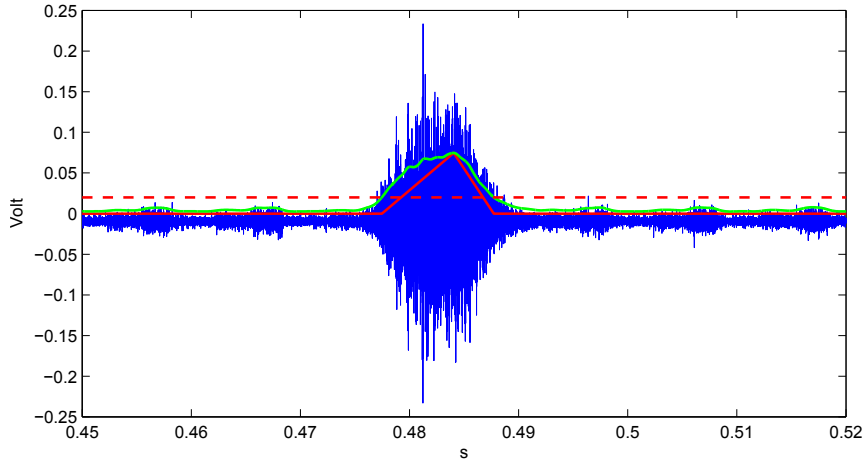


Figure 4: Construction of the *TriSignal* from the AE envelope. Color legend: raw AE (blue); AE envelope (green); *TriSignal* (solid red); static threshold (dashed red).

2.2 *TriSignal* in the time domain

The most challenging part in building the *TriSignal* is determining when each AE Burst starts and when it ends. This is also a crucial point within the method, because the results that can be obtained from the *TriSignal* are highly dependent on the correct description of the bursts. The easiest way to perform this is by defining a static threshold and an hysteresis parameter to avoid the division of a single burst into several bursts of shorter duration. With this method, the beginning and end of each burst are determined by the times of threshold crossing meeting the hysteresis criteria. This method can be applied to the raw AE, as it was presented in Fig.3 or to a filtered version of the raw AE signal, where the filter is used to enhance the burst with respect to the background noise and improve the burst detection process. Spectral Kurtosis [15][16] or Cyclostationarity-based quantities (e.g. SCD, SCoh) can be computed from a short portion of the AE-signal containing some bursts for identification of the optimum filtering range. Depending on the characteristics of the background noise, a moving threshold could be a better alternative. This can be a moving RMS or a similar quantity.

Alternatively, the method can be applied to the envelope of the AE, as presented in Fig.4. The envelope being a measure of the energy flow in time, it usually results more practical to detect the bursts on the envelope of the AE. In this case, it must be considered that the values obtained for each triangle (i.e. t_s^i , t_m^i and y_m^i) correspond to values of the energy flow rather than values of the actual AE signal.

The choice of the most appropriate method for burst detection, as well as the selection of the hysteresis parameters will depend on the individual characteristics of the AE signal being measured; more precisely, on the specific features of the bursts with respect to the continuous part of the signal. We have found the detection based on the crossing of the AE envelope across a fixed threshold to have acceptable results in the experiments we have conducted till date, which include AE from faulty bearings, from the meshing of spur gears and from hydraulic motors.

The benefits of the *TriSignal* are not only the data reduction, but the quantities that can be obtained from it. For example, it is possible to calculate estimators of time-domain scalar values typically determined from the raw AE, such as the peak value, rise time (equal to $t_m^i - t_s^i$), fall time (equal to $t_e^i - t_m^i$), event duration (equal to $t_e^i - t_m^i$), number of bursts, event density, etc. Other scalar values such as the RMS and Kurtosis cannot be estimated from the *TriSignal* because the information of the background noise is not contained. If these (and/or other) values are required, it would be necessary to calculate them from the raw AE and store them together with the *TriSignal*. Note the information of each of these values is available for each burst, so it is even possible to scrutinize their statistics through, for example, their probability density functions.

As a completely synthetic signal, it is possible to use the results from the scalar values of each burst for filtering or source separation purposes. Consider, for example, an AE signal containing two families of repetitive bursts from two different sources. Both sources generate bursts having the same frequency range, but one of them produce bursts with larger duration. In a case like this, the event duration scalar value for each triangle can be used to discriminate between a burst coming from one or the other source. This process leads to the construction of two *TriSignals*, one for each source, which can be analyzed separately. Figure 5 shows a similar

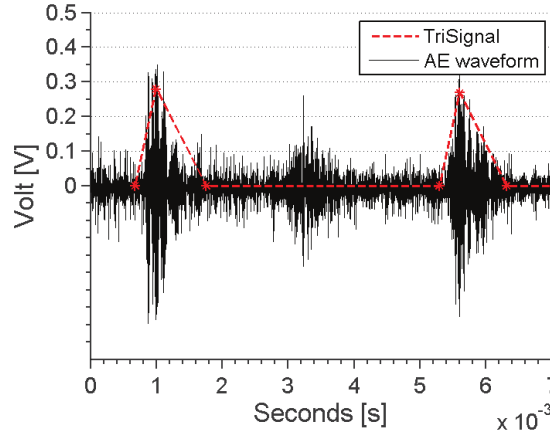


Figure 5: *TriSignal* used for separation of AE bursts from different sources (*TriSignal* determined from the AE envelope).

example in which the peak value was used to discriminate between two sources; the *TriSignal* shown contain only the triangles with peak value higher than 0.25 V.

2.3 *TriSignal* in the frequency domain

Once the *TriSignal* has been constructed, a natural step forward consist in the inspection of its periodicities. In the case of the traditional envelope, this is usually done by scrutinizing the envelope magnitude spectrum, which is obtained by calculation of the Fourier transform of the envelope signal. Considering its characteristics, it is logical to proceed similarly with the *TriSignal*. However, this is not as straightforward, since from its definition, the *TriSignal* is an unevenly sampled signal. As such, it does not meet the requirements for the calculation of the magnitude spectrum by direct computing its Fourier transform. This issue can be solved by using some methods. The most simple would be interpolating the *TriSignal* so as to have an evenly-sampled version of it, and then calculate its Fourier transform. However, as reported by [17], this method performs poorly especially if the signal presents long spacing between successive points, as is the case for the *TriSignal*. The Lomb-Scargle normalized periodiogram (Lomb spectrum in what follows) is another possible method which is not subjected to this problem. It is based on the evaluation of sines and cosines of different frequencies together with the unevenly sampled signal only at the times corresponding to the points of the latter [17]. That is, in the case of the *TriSignal*, at the times t_s^i , t_m^i and t_e^i for all hits of the signal portion under analysis. We call the spectrum obtained from the calculation of the Lomb Spectrum of the *TriSignal*, the *TriSpectrum*, which results in an estimator of the shape and therefore the frequency distribution of the AE envelope.

After calculation of the mean μ and variance σ^2 of all data points of the *TriSignal*, the *TriSpectrum* $G_{yy}(f)$ is calculated by

$$G_{yy}(f) = \frac{1}{2\sigma^2} \left\{ \frac{\left[\sum_i \sum_j (t_j^i - \mu) \cos 2\pi f (t_j^i - \tau) \right]^2}{\sum_i \sum_j \cos^2 2\pi f (t_j^i - \tau)} \right\} + \frac{1}{2\sigma^2} \left\{ \frac{\left[\sum_i \sum_j (t_j^i - \mu) \sin 2\pi f (t_j^i - \tau) \right]^2}{\sum_i \sum_j \sin^2 2\pi f (t_j^i - \tau)} \right\} \quad (1)$$

where i is the burst index, and $j = s, m$, and e . The frequency-dependent time constant τ is defined by

$$\tan 4\pi f \tau = \frac{\sum_i \sum_j \sin 2\pi f t_j^i}{\sum_i \sum_j \cos 4\pi f t_j^i} \quad (2)$$

where f is the frequency in Hz.

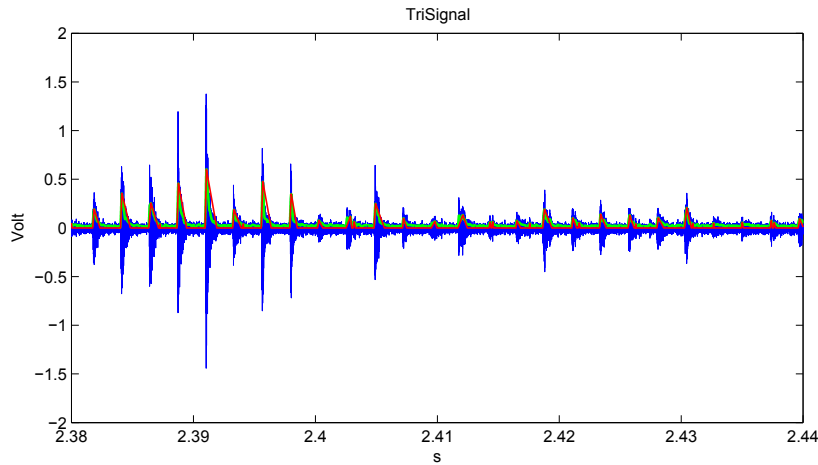


Figure 6: Portion of *TriSignal*, non-faulty planetary gearbox. Color legend: raw AE (blue); AE envelope (green); *TriSignal* (red).

The Lomb spectrum is then obtained with a low-frequency limit of $f_{\text{low}} = 1/T$, where T is defined as the total time-span between all data points of the *TriSignal* considered for the calculation (i.e. $T = \max\{t_j^i\} - \min\{t_j^i\}$). Since it is highly probable that some data points of the *TriSignal* will be spaced much closer than the average spacing considering all data points, it is even possible to obtain statistically significant results in the Lomb spectrum for frequencies above the Nyquist frequency that would be obtained should all data points be equally-spaced in the considered time-span T . The Lomb spectrum algorithm presented is a slow algorithm; however, an approximation of it can be calculated much faster by making use of the FFT algorithm [17].

Following, we present an example of the use of the *TriSpectrum* calculated from the AE signal measured on a single-stage spur-gear planetary gearbox. The gearbox has three equally spaced planet gears, each with 26 teeth. The sun gear has 18 teeth and the annulus gear has 72 teeth. The gearbox is used in reduction mode with a rotational speed of the sun gear of $f_S = 30$ Hz and a constant load of 65 Nm is applied to the output of the transmission. This gearbox pertains to group A according to the classification proposed in [4]: *Planetary gearboxes with equally-spaced planet gears and in-phase gear meshing processes*, so that the meshing of all wheels inside the gearbox produce the burst part of the AE activity at the same time. For $f_S = 30$ Hz, the gear mesh frequency is 432 Hz and the rotational speed of the carrier plate is 6 Hz.

Acoustic emissions were measured with a sensor installed on the outer part of the annulus gear. The *TriSignal* was constructed based on the envelope of the measured AE, as shown in Fig.6. The *TriSpectrum* was calculated from the *TriSignal* using the previously defined methodology; the portion around the first gear mesh harmonic is presented in Fig.7a. The modulations observed as sidebands around the gear mesh frequency (marked with \times) are due to the varying transfer path between the source position of the AE (which continuously changes during operation of the gearbox) and the (fixed) position of the sensor. The components recognized in the *TriSpectrum* are thus normal for a gearbox of these characteristics and, therefore, the diagnosis is good condition of the unit. For comparison purposes the envelope spectrum of the AE is shown in Fig.7b. Note the similarity with the shape of the *TriSpectrum*. The numeric cursors in figures 7a and 7b are referenced in the next paragraph.

A localized defect was seeded in one tooth of one planet gear. The defect was accomplished using an electrical engraving machine, Fig.8, and is considered a surface defect over the complete flank of one tooth. The measurement was taken in the same manner described previously and the same procedure was followed to obtain the *TriSignal* and the *TriSpectrum*. These are shown in Fig.9 and Fig.10a, respectively. The *TriSpectrum* now reveals components not present before, marked with the numeric cursors. The space between each of these components and the gear mesh frequency equals the relative rotational frequency of the planet gear with respect to the carrier plate, which in this case is $f_{p|c} = 16.6$ Hz. Their presence is indicative of the defect (note they were not present in the non-faulty situation, see cursors in Fig.7a and Fig.7b). The envelope spectrum is shown in Fig.10b, from which again the same information offered by the *TriSpectrum* is obtained.

In both faulty and non-faulty case, a signal length of 18 seconds was used. The raw AE was sampled at a rate of 2.5 MHz. In a double-precision format each of these signals uses 360 MByte. The envelope has

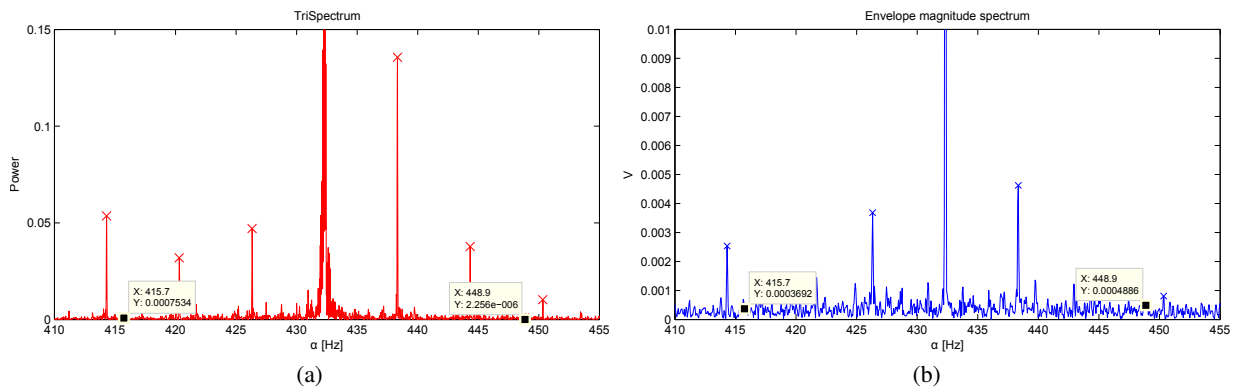


Figure 7: Portion around the first gear mesh harmonic of the (a) *TriSpectrum* and (b) envelope spectrum. Non-faulty planetary gearbox.



Figure 8: Localized defect in one planet gear wheel.

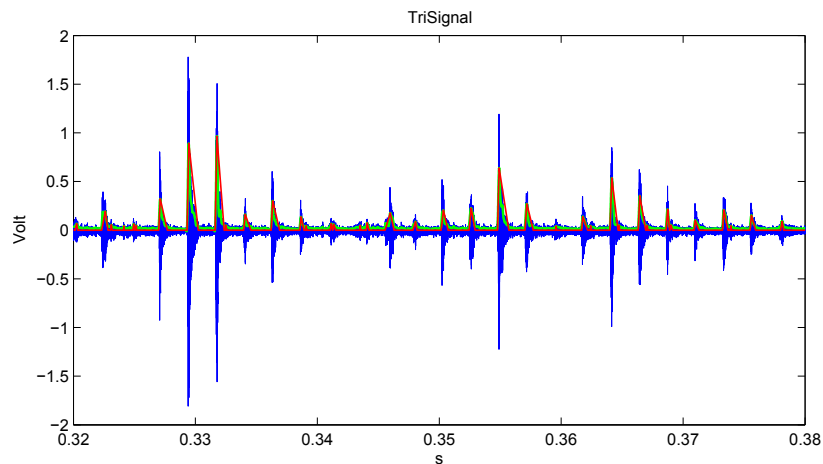


Figure 9: Portion of *TriSignal*, faulty planetary gearbox. Color legend: raw AE (blue); AE envelope (green); *TriSignal* (red).

been downsampled to 10 kHz, for which a storage space of 1.44 MByte is needed. In the non-faulty case, the *TriSignal* has 11262 triangles occupying a storage space of 0.36 MByte. In the faulty case, the *TriSignal* has 10591 triangles and uses 0.34 MBytes. This represents an average data reduction of 99.9% with respect to the raw AE, and of 75.7% with respect to the envelope.

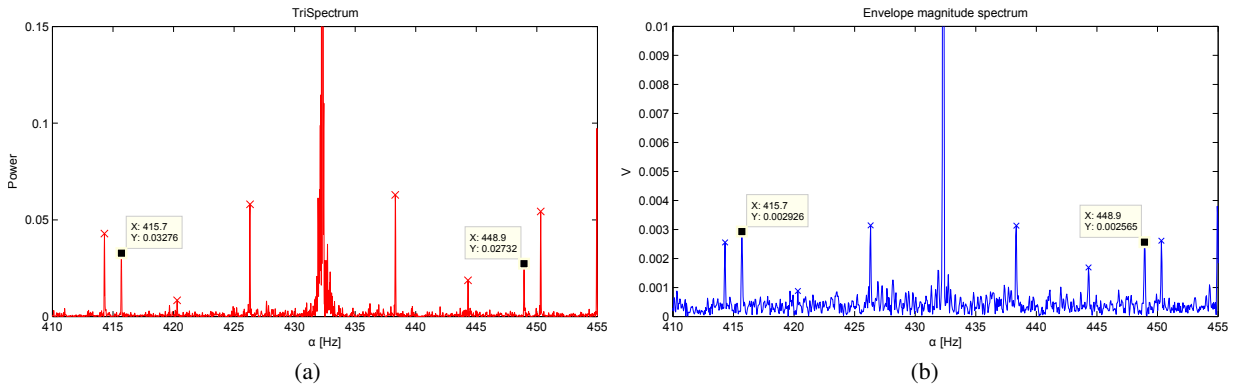


Figure 10: Portion around the first gear mesh harmonic of the (a) *TriSpectrum* and (b) envelope spectrum. Faulty planetary gearbox.

3 Some final remarks

The *TriSpectrum* appears as an interesting alternative to the envelope spectrum. However, the latter is –of course– preferred; if there are enough resources to base the monitoring in the envelope, then this should be preferred. The only idea behind the *TriSignal* and the *TriSpectrum* is to provide an alternative to the envelope when it is desired to keep the minimum stored data.

We finally emphasize again the critical importance of detecting the bursts correctly on the construction of the *TriSignal*. Considering that different mechanical systems have specific features, a previous analysis of the AE of each particular case will be, in general, necessary. In cases where the bursts are clearly observable in the signal, this represents no problem. In other cases, it might be needed to perform certain analysis to define a filter which better isolate the bursts from the rest of the signal. If the mechanical system produce bursts in the non-faulty condition (e.g. in gears), then a filter defined to isolate the normal bursts would be a good choice. The hypothesis here is that the bursts generated by a fault-related source will probably share the same frequency range or at least part of it, which is often the case. On the other hand, if the system does not produce bursts in the non-faulty condition (e.g. in bearings), a resonant zone of the sensor can be chosen. Alternatively, measurements can be done while generating artificial AE sources on the case of the machine and then selecting a filter by analyzing its frequency content. The artificial AE source can be generated in practice by impacting the case with a screwdriver or by breaking a graphite pencil lead on the case of the machine.

Alternatives to select the most appropriate filter include Spectral Kurtosis and cyclostationary-based tools, although less sophisticated techniques can be used in some cases. For example, the dB spectrum difference can be used using two portions of the same signal, one including one or more bursts and the other including only the continuous part. Fig.11 illustrates this method applied on the AE signal measured on the hydraulic motor. Note in this case it is actually not necessary to use any method, because the bursts are clearly visible in the raw AE signal. Still, the method results in a signal where the bursts are even more evident. Note also how the amplitude modulation present in the portion between the bursts has also been removed. The amplitude modulation is due to electronic interference and, therefore, is not real AE. Since the interference is present in both signal portions, the dB spectrum difference is maximum in the frequency region where the AE burst predominates.

4 Conclusions

A method for data reduction of acoustic emissions has been presented, which additionally retains the key information for machine failure diagnosis. The method consists in the construction of the *TriSignal*, a synthetic signal enveloping the characteristic bursts present in the raw AE. In some of the examples shown, the reduction was of 99.997% with respect to the raw AE signal, and of 99.440% with respect to the envelope of the AE. Further processing of the *TriSignal* using the Lomb-Scargle periodogram results in the *TriSpectrum*, which is an estimator of the frequency structure of the envelope and, therefore, a valuable tool for failure diagnosis. The most important part of the method relies in the correct identification of the bursts. Previous to the application of the method on a particular case, an study should be preformed to analyze the characteristics of the AE and

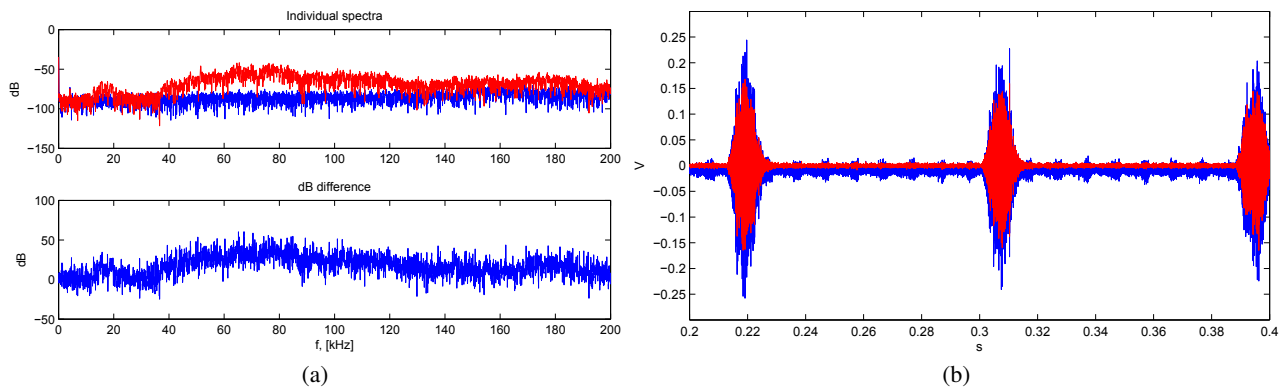


Figure 11: dB spectrum difference method used to improve signal-to-noise ratio of the AE signal. (a) Top: individual spectra of portion including burst (red) and portion not including burst (blue); bottom: dB spectrum difference. (b) Raw AE signal (blue) and filtered AE signal (red).

find the filter which maximizes the presence of the bursts with respect to the rest of the signal.

Acknowledgements

The first author thanks FONDECYT for the support of the Project 11110017.

References

- [1] D. Mba and Raj B.K.N. Rao, *Development of acoustic emission technology for condition monitoring and diagnosis of rotating machines; bearings, pumps, gearboxes, engines and rotating structures*, The Shock and Vibration Digest, 38(1), 2006.
- [2] C. Tan and D. Mba, *Correlation between acoustic emission activity and asperity contact during meshing of spur gears under partial elastohydrodynamic lubrication*, Tribology Letters, 20(1) pp.63-67, September 2005.
- [3] R.I. Raja Hamzah and D. Mba, *The influence of operating condition on acoustic emission (ae) generation during meshing of helical and spur gear*, Tribology International, 42(1) pp.3-14, 2009.
- [4] Vicuña CM, *Effects of operating conditions on the Acoustic Emissions (AE) from planetary gearboxes*, Appl Acoust (2013), <http://dx.doi.org/10.1016/j.apacoust.2013.04.017>.
- [5] Álvaro Barrueto Novoa, Cristián Molina Vicuña, *New aspects concerning the generation of Acoustic Emissions (AE) in spur gears and the influence of operating conditions*, Surveillance 7, Chartres, France, 2013 October.
- [6] D.G. Aggelis, E.Z. Kordatos, T.E. Matikas, *Acoustic emission for fatigue damage characterization in metal plates*, Mechanics Research Communications 38 (2011) pp.106-110.
- [7] N. Tandon, G.S. Yadava, K.M. Ramakrishna, *A comparison of some condition monitoring techniques for the detection of defect in induction motor ball bearings*, Mechanical Systems and Signal Processing 21 (2007) pp.244-256.
- [8] A. Choudhury, N. Tandon, *Application of acoustic emission technique for the detection of defects in rolling element bearings*, Tribology International 33 (2000) pp.39-45.
- [9] A Morhain and D Mba, *Bearing defect diagnosis and acoustic emission*, Proc. Instn Mech. Engrs Vol. 217 Part J: J. Engineering Tribology, pp.257-272, 2003.

- [10] N. Tandon and B. C. Nakra, *Defect Detection in Rolling Element Bearings by Acoustic Emission Method*, Journal of Acoustic Emission, Volume 9, Number 1, pp.25-28, 1990.
- [11] Saad Al-Dossary, R.I. Raja Hamzah, D. Mba, *Observations of changes in acoustic emission waveform for varying seeded defect sizes in a rolling element bearing*, Applied Acoustics 70 (2009) pp.58-81.
- [12] Abdullah M. Al-Ghamd, David Mba, *A comparative experimental study on the use of acoustic emission and vibration analysis for bearing defect identification and estimation of defect size*, Mechanical Systems and Signal Processing 20 (2006) pp.1537-1571.
- [13] Jérôme Antoni, *Cyclic spectral analysis in practice*, Mechanical Systems and Signal Processing 21 (2007) pp.597-630.
- [14] R.B. Randall, J. Antoni, S. Chobsaard, *The relationship between spectral correlation and envelope analysis in the diagnostics of bearing faults and other cyclostationary machine signals*, Mechanical Systems and Signal Processing (2001) 15(5) pp.945-962.
- [15] Dwyer, R., *Detection of non-Gaussian signals by frequency domain Kurtosis estimation*, Acoustics, Speech, and Signal Processing, IEEE International Conference on ICASSP '83. (Volume:8), pp.607-610, 1983.
- [16] Jérôme Antoni, *The spectral kurtosis: a useful tool for characterising non-stationary signals*, Mechanical Systems and Signal Processing 20 (2006) pp.282-307.
- [17] William H. Press, Saul A. Teukolsky, William T. Vetterling, Brian P. Flannery, *Numerical Recipes: The Art of Scientific Computing*, Cambridge University Press; 3rd edition, ISBN: 978-0521880688, 2007.